HHS Public Access

Author manuscript

Nat Commun. Author manuscript; available in PMC 2014 December 05.

Published in final edited form as:

Nat Commun. ; 5: 5482. doi:10.1038/ncomms6482.

Ciliary membrane proteins traffic through the Golgi *via* aRabep1/GGA1/Arl3-dependent mechanism

Hyunho Kim[1], **Hangxue Xu**[1], **Qin Yao**[1], **Weizhe Li**[1], **Qiong Huang**[1], **Patricia Outeda**[1], **Valeriu Cebotaru**[2], **Marco Chiaravalli**[3], **Alessandra Boletta**[3], **Klaus Piontek**[2], **Gregory G Germino**[4], **Edward J Weinman**[1], **Terry Watnick**[1], and **Feng Qian**[1]

[1]Department of Medicine, Division of Nephrology, University of Maryland School of Medicine, Baltimore, Maryland, 21201, USA

[2]Department of Medicine, The Johns Hopkins University School of Medicine, Baltimore, MD, 21205, USA

[3]Division of Genetics and Cell Biology, San Raffaele Scientific Institute, 20132, Milan, Italy

[4]National Institute of Diabetes and Digestive and Kidney Disease, National Institute of Health, Bethesda, Maryland, 20892, USA

Abstract

Primary cilia contain specific receptors and channel proteins that sense the extracellular milieu. Defective ciliary function causes ciliopathies such as autosomal dominant polycystic kidney disease (ADPKD). However little is known about how large ciliary transmembrane proteins traffic to the cilia. Polycystin-1 (PC1) and-2 (PC2), the two ADPKD gene products, are large transmembrane proteins that colocalize to cilia where they act to control proper tubular diameter. Here we describe that PC1 and PC2 must interact and form a complex to reach the *trans*-Golgi network (TGN) for subsequent ciliary targeting. PC1 must also be proteolytically cleaved at a GPS site for this to occur. Using yeast two-hybrid screening coupled with a candidate approach, we identify a Rabep1/GGA1/Arl3-dependent ciliary targeting mechanism, whereby Rabep1 couples the polycystin complex to a GGA1/Arl3-based ciliary trafficking module at the TGN. This study provides novel insights into the ciliary trafficking mechanism of membrane proteins.

Corresponding author; Feng Qian, University of Maryland School of Medicine, Bressler Research Building 2-017A, 655 W. Baltimore St. Baltimore, MD 21201, USA. Tel: +1 410 706 5804, Fax: +1 410 328 5685, fqian@medicine.umaryland.edu.
Qin Yao and Weizhe Li contributed equally to this work.

Contributions

F.Q. developed the concept of this study. H.K., H.X., Q.Y., W.L., Q.H., P.O., V.C., M.C., A.B., K.P., G.G.G., E.J.W., T.W., and F.Q. designed and performed experiments and analysed data. H.K. and F.Q. prepared the draft and final version of the manuscript. All authors read and approved the final manuscript.

Competing interests statement

The authors declare that they have no competing financial interests.

Note: Supplementary Information is available on the Nature Communications website.

INTRODUCTION

Primary cilia are microtubule-based non-motile projections on the apical surface of cells, which organize important signaling pathways mediated by specific receptors and channel proteins at the ciliary membrane in response to mechanical and chemical stimuli[1]. They are the key organelle for controlling correct tubular diameter, and defective ciliary function causes a variety of ciliopathies[1], including autosomal dominant polycystic kidney disease (ADPKD)[2, 3]. The ciliary membrane is separated from the plasma membrane by apericiliary diffusion barrier[4] and ciliary membrane proteins must be transported to the cilia from their site of synthesis in the rough endoplasmic reticulum (ER) for proper ciliary function[5]. Experimental evidence favors a targeted delivery model whereby ciliary membrane proteins are sorted in the Golgi and are targeted to the cilium by a vesicular pathway[5]. Numerous protein complexes have been implicated in polarized trafficking of post-Golgi vesicles to cilia, including the BBSome[5] and IFT complexes[6]. However, the mechanism by which transmembrane proteins are sorted for ciliary trafficking is poorly understood.

Polycystin-1 (PC1) and polycystin-2 (PC2), the two ADPKD gene products[7, 8] are large transmembrane proteins that co-localize to cilia[9, 10] where they play an important role in calcium-based signaling[2, 11]. Loss of polycystin function in cilia is implicated in cyst formation[2]. PC1 is a4,302-amino acids (aa) atypical adhesion G-protein coupled receptor (aGPCR) with 11-transmemrbane domains[12, 13]. A fundamental property of PC1 is *cis*-autoproteolytic cleavage at ajuxta membrane G-protein coupled receptor cleavage site (GPS)[14, 15, 16]. GPS cleavage of PC1 is developmentally regulated in the kidney, whereby PC1 is largely uncleaved in early embryonic kidneys but becomes extensively cleaved after birth[17, 18]. Mice with a “knock-in” missense amino acid substitution that disrupts GPS cleavage (*Pkd1*$^{V/V}$ mice) express non-cleavable PC1 (PC1^{V}) and develop cystic kidney disease during the postnatal period[15]. As shown for other a GPCRs, cleavage results in a heterodimeric PC1 form, in which the N-terminal fragment (PC1$_{NTF}$) remains stably and non-covalently associated with the transmembrane C-terminal fragment (PC1$_{CTF}$)[14, 19]. More recently, we have shown that GPS cleavage generates a complex pattern of endogenous PC1 forms but is not *per se* required for PC1 to move to the Golgi[18]. How GPS cleavage affects trafficking and function of PC1 or other a GPCR s*in vivo* remains unclear.

PC2 is a 968-aa long 6-transmembrane-spanning transient receptor potential channel family member that acts as a calcium release channel and is most abundantly distributed to the ER[20, 21]. PC1 and PC2 form a receptor/channel complex by direct interaction *via* coiled-coil domains in their cytoplasmic C-termini[22, 23, 24]. Several studies have reported that this interaction is required for surface membrane localization of the complex in certain, but not in all, cell types[25, 26, 27]. However, there is disagreement as to whether the interaction is necessary for ciliary localization since each protein has its own ciliary targeting signal[25, 28, 29]. In some studies,PC2 was able to localize to cilia independently of PC1[28, 30], while others studies show that this requires PC1[2, 25, 31, 32]. In addition, PC1 and PC2 may take different routes to reach the cilium. PC1 is described to traffic to cilia from the *trans*-Golgi network (TGN) *via* post-Golgi vesicles in an Arf4-dependent process[29]. However, PC2 was reported to move to the cilium directly from the *cis*-Golgi compartment without traversing the Golgi apparatus[30].

In this report, we use a comprehensive approach to define the ciliary trafficking mechanism of endogenous polycystins in polarized ciliated renal epithelial cells. We demonstrate that PC1-PC2 interaction and GPS cleavage of PC1 are both required for the polycystin complex to reach the TGN and for subsequent ciliary targeting. We use yeast two-hybrid screening coupled with a candidate approach to identify a novel protein complex composed of Rabep1, GGA1 and Arl3, which is responsible for the sorting and targeting of the polycystin complex to the cilium. Our study provides novel insights into the ciliary trafficking mechanism of transmembrane proteins, with implications for ADPKD, the most common human ciliopathy.

RESULTS

Polycystin complex is required for ciliary localization

We used several strategies to determine whether native PC1 and PC2 might regulate each other's ciliary localization *in vivo*. We found that PC1 localizes to cilia in wild-type mouse embryonic fibroblasts (MEFs), but not in *Pkd2*$^{-/-}$ MEFs (Fig. 1a, c). PC2 also localizes to cilia in wild-type MEFs, but not in *Pkd1*$^{-/-}$ MEFs (Fig. 1b, c). Furthermore, exogenous mouse PC1 expressed in *Pkd1*$^{-/-}$ MEF cells trafficked to the cilia and concomitantly restored ciliary localization of endogenous PC2 (Fig. 1d). The rescue of ciliary PC2 localization was not seen when GFP was expressed (Supplementary Fig. 1). We then used shRNA to knock down endogenous *Pkd2* expression in DBA-positive collecting duct (CD)-derived cells[15] and we found that the ciliary localization of PC1 was abolished (Fig. 1e). Likewise, the ciliary localization of PC2 was not detectable when *Pkd1* expression was knocked down (Fig. 1f). The interdependence of PC1 and PC2 ciliary localization was confirmed in IMCD cells with stable expression of full-length epitope-tagged mouse PC1 (IMCD^{PC1WT}, Supplementary Fig. 2a-e). In mice with a floxed *Pkd1* allele, PC2 was absent in the cilia of cystic kidney tubules after post-natal *Pkd1* inactivation[33] while the protein was detected in the cilia of the normal tubular epithelial cells (Fig. 1g).

We then tested whether direct interaction of PC1 and PC2 was required for ciliary localization of the polycystin complex. In MDCK cells with stable and inducible expression of epitope-tagged wild-type mouse PC1 (MDCK^{PC1WT}, Table 1), we confirmed that recombinant PC1 formed a complex with endogenous PC2 (Fig. 2a, b). We found that, upon induction of its expression, PC1 trafficked to cilia and concomitantly induced ER-resident endogenous PC2 to translocate to cilia as well (Fig. 2c-e). We disrupted the interaction of PC1 and PC2 by introducing amino acid substitutions at two strategic positions (L4219P and A4222P) within the coiled-coil domain[22, 24](PC1^{2M}) (Fig. 2a, b). In contrast to wild-type PC1 (Fig. 2f), we found that PC1^{2M} did not traffic to the cilia, and did not induce endogenous PC2 to translocate to the cilia(Fig. 2g,i).Similarly,PC1^{R4218X}(R/X) mutant[34], which corresponds to an ADPKD patient-derived truncating mutant R4227X lacking the intact coiled-coil domain[22, 27], did not interact with endogenous PC2 (Fig 2a, b) and failed to cause PC2 to translocate to cilia (Fig. 2h,i). Taken together, our results show that PC1 and PC2 must interact and form a complex for ciliary localization to occur in renal tubular epithelial cells.

Polycystin complex is required to reach the Golgi apparatus

We next analyzed the *N*-glycosylation pattern of the polycystin complex to investigate how it travels through the cell. EndoH cleaves high-mannose *N*-glycans attached in the ER, but not the *medial*/*trans*-Golgi-modified complex *N*-glycans[35]. EndoH resistance is thus indicative that glycoproteins have reached the *medial*/*trans*-Golgi compartment. Endo genous PC1 was immunoprecipitated with anti-CC (Fig. 2a) from MEFs and the resulting precipitate was treated with EndoH followed by analysis with SDS–PAGE and Western blotting. In wild-type MEFs, PC1 was predominantly present as GPS-cleaved forms, which are recognized as the EndoH-resistant ("Cleaved-R") and-sensitive ("Cleaved-S") $PC1_{NTF}$ bands (Fig. 3a, upper panel, lanes 2–4/2′-4′) as previously described[18]. Under these conditions, we observed very low levels of uncleaved PC1. In the whole-cell lysate, PC2 was detected as a single 120-kDa band (lower panel, lane 1/1′) as previously shown[20, 21]. However, the fraction of PC2 that is co-immunoprecipitated with PC1 appeared as two distinct bands of similar intensity (lane 2/2′). Treatment of this PC2 fraction with EndoH revealed that the upper band (130-kDa, $PC2_{130}$) was EndoH resistant, whereas the lower band (120-kDa, $PC2_{120}$) was EndoH sensitive (lane 4/4′). A similar pattern was found in both kidney tissues and CD cells (Fig. 3b). These results identify a significant amount of EndoH-resistant pool of polycystin complex *in vivo*. In *Pkd2*$^{-/-}$ MEFs, GPS-cleaved PC1 remained entirely EndoH-sensitive (Fig. 3a, upper panel, lanes 5–7), implying that PC1 cannot reach the *trans*-Golgi without PC2. Likewise, in CD cells with *Pkd2* knockdown, cleaved PC1 remains EndoH sensitive (Fig. 3c). Together, these data indicate that PC1 and PC2 form a complex in the ER and that direct inter action is required for the complex to reach the Golgi apparatus.

Polycystin complex traffics to cilia through the Golgi

In order to determine intracellular trafficking of ciliary PC1 and PC2, we isolated intact cilia from MDCK cells similarly as previously described[36] (Fig. 4a) and analyzed their *N*-glycosylation patterns. The preparation contained intact cilia as visualized by IF microscopy with a ciliary marker (Fig. 4b). Moreover, Western blot analysis of this ciliary preparation detected acetylated-tubulin and Polaris (known ciliary proteins), but not β-actin (an abundant cytoskeletal protein), Alix (an abundant component of exosome proteomes)[37], c-Met (an apical plasma membrane protein)[38] or IGFBP-2(a secreted protein)[39](Fig. 4b). These results thus validated that the cilium preparation did not contain a detectable amount of contamination from intracellular and secreted proteins, exosomes or plasma membrane. We detected a single ~450-kDa PC1 band in the cilium preparation from induced $MDCK^{PC1WT}$ cells (Fig. 4c, upper panel, lane 3), but not from un-induced cells (lane 2) or $MDCK^{pcDNA5}$ control cells (data not shown). The ciliary PC1 migrated between the uncleaved PC1 and cleaved PC1 detected in the same cells stripped of cilia (cell body) (lane 1). Ciliary PC1 was resistant to EndoH (lane 3), but migrated at the expected MW of cleaved $PC1_{NTF}$ (~370-kDa)[14] after removal of *N*-glycan by PNGaseF treatment (Fig. 4d, upper panel, lanes 2 and 5). This result identified the ciliary PC1 as the cleaved EndoH-resistent form. The uncleaved PC1 was absent in the cilia but it was present at similar levels as cleaved PC1 in the cell body. These results indicate that only cleaved PC1 reaches the cilia and that it traffics through the Golgi. Remarkably, we detected a PC2 band of a MW of ~130-kDa in the cilium

preparation from induced MDCK^{PC1WT} cells (Fig. 4c, lane 3), which migrated slower than the ~120-kDa PC2 band detected in the whole cell body lysate (lane 1). The ciliary PC2 was also resistant to EndoH (Fig. 4d, lane 6) and migrated at the expected MW of PC2 after PNGaseF treatment (lane 5), as the $PC2_{130}$ seen in endogenous polycystin complex from native tissues and cells (Fig. 3). Taken together, the presence of exclusively EndoH-resistant PC1 and PC2 in the cilia provides direct biochemical evidence that the polycystin complex traffics to cilia through the Golgi apparatus.

Ciliary trafficking of polycystins requires GPS cleavage

The absence of uncleaved PC1 in the cilia suggests that GPS cleavage is required for ciliary trafficking of the polycystin complex. In order to test this we asked whether the non-cleavable $PC1^{V}$ could be found in cilia. In fact we were unable to detect either ciliary $PC1^{V}$ or PC2 in the cilia of collecting duct cells derived from *Pkd1*$^{V/V}$ kidneys ($CD^{V/V}$)(Fig. 5a). In addition, recombinant $PC1^{V}$ overexpressed in MDCK ($MDCK^{PC1V}$, Table 1) was unable to reach the cilia and did not induce endogenous PC2 to translocate to cilia (Fig. 5b). We obtained similar results in $IMCD^{PC1V}$ cells (Supplementary Fig. 2f). Consistent with this result, we were unable to detect either $PC1^{V}$or PC2 in the cilium preparation from induced $MDCK^{PC1V}$ cells by Western blot analysis (data not shown). Importantly, PC2 was not detectable in the cilia of cystic tubules of the *Pkd1*$^{V/V}$ kidneys (Fig. 5c).

To investigate the basis of the observed requirement of GPS cleavage, we analyzed the *N*-glycosylation pattern of the polycystin complex in *Pkd1*$^{V/V}$ MEFs versus wild-type MEFs (Fig. 5d). Then on-cleavable $PC1^{V}$ was immunoprecipitated from *Pkd1*$^{V/V}$ MEFs as an ~600-kDa EndoH-resistant band ($PC1^{V\text{-}600}$) and an ~520-kDa EndoH-sensitive band ($PC1^{V\text{-}520}$)(upper panel, lanes 4–6). We found that PC2 was still co-precipitated by $PC1^{V}$, but the co-precipitated PC2 appeared only as an ~120-kDa band and was completely sensitive to EndoH (i.e., $PC2_{120}$, lanes 4–6), lacking the EndoH-resistant $PC2_{130}$ seen in WT MEFs (lanes 1–3). The same *N*-glycosylation pattern was found for the polycystin complex in *Pkd1*$^{V/V}$ kidney tissues (Fig. 5e). These results imply that only the EndoH- sensitive $PC1^{V\text{-}520}$, but not the EndoH-resistant $PC1^{V\text{-}600}$, is associated with PC2 in the *Pkd1*$^{V/V}$ samples. Our data collectively show that GPS cleavage is required for the ciliary localization of the polycystin complex by enabling its trafficking to the *trans*-Golgi compartment. In the absence of cleavage, the $PC1^{V}$/PC2 complex cannot reach the *trans*-Golgi.

Rabep1 binds PC1C-terminus for ciliary trafficking

To identify the molecules that mediate polycystin complex ciliary trafficking, we performed a yeast two-hybrid screen for PC1 interacting proteins using the entire 215-amino acid C-terminal tail as bait. Thirteen unique cDNA clones were identified that specifically interact with the PC1 C-terminus. One of these clones corresponded to amino acids 465 to 799 of Rabep1 (Fig. 6a), an effector of multiple Rab GTPases involved in various steps of intracellular vesicular trafficking[40]. This protein was chosen for further analysis. We used mutational analysis to map the Rabep1 interaction region (Fig. 6b) and showed that the C-terminal 89 amino acids containing the intact coiled-coil domain of PC1 (PC1-M1/M2) was sufficient for interaction with Rabep1. The binding sites for Rabep1 and PC2 overlap but are

not identical, because the C-terminal 41 aa of PC1 (PC1-M3) was required for Rabep1 interaction, but not for PC2.

We confirmed that the PC1-Rabep1 interaction occurs *in vivo* by demonstrating co-immunoprecipitation from CD cells (Fig.6c). We were unable to co-immunoprecipitate these two proteins from CD cells with *Pkd1* knockdown (Fig. 7a) nor from *Pkd1*$^{\Delta CMYC/\Delta CMYC}$ knock-out embryos expressing Myc-tagged truncated PC1[41] (Fig. 7b). We found that the PC1-Rabep1 interaction occurred in *Pkd2* null MEFs (Fig. 7c). This suggests that PC1 binds Rabep1 in a pre-Golgi compartment since PC1 does not exit the ER in the absence of PC2 (Fig. 3a).

Next we tested whether Rabep1 was required for ciliary localization of the polycystin complex. We used shRNA to knockdown Rabep1 in CD cells and this abolished ciliary localization of PC1 and PC2 (Fig. 7d, e). Rabep1 knockdown in the CD cells, however did not affect formation of the polycystin complex nor its acquisition of EndoH resistance (Fig. 7f, lane 2), indicating that Rabep1 is not required for the polycystin complex to reach the Golgi. Collectively, these results show that Rabep1 binds to the distal portion of $PC1_{CTF}$'s C-terminal tail and suggest that Rabep1 likely plays a critical role for ciliary targeting of the polycystin complex at the TGN by recruiting ciliary targeting machinery.

Rabep1 recruits polycystin complex to GGA1 and Arl3 at TGN

Rabep1 has been shown to interact with GGA1[42, 43, 44] (Golgi-localized, gamma adaptin ear-containing, ARF-binding) in the context of fusion of TGN-derived vesicles with endosomes[45]. GGA1 is an effector of Arf GTPases at the TGN and mediates protein sorting and vesicle budding from the TGN[43, 46]. We therefore hypothesized that polycystin complex-associated Rabep1 might bind GGA1, which in turn might mediate the ciliary sorting of the complex. Indeed, we found that PC1 can co-immunoprecipitate GGA1, along with PC2 and Rabep1, from CD cell lysates (Fig. 7a, f) and *Pkd1*$^{MYC/MYC}$ embryos (Fig. 7b). GGA1 knockdown abolished the ciliary localization of both PC1 and PC2 in CD cells (Fig. 7d, e), without affecting the acquisition of EndoH-resistance of the polycystin complex (Fig. 7f, lane 3). PC1-GGA1 interaction was abolished by Rabep1 knockdown (lane 2), whereas PC1-Rabep1 interaction still occurred when GGA1 was knocked down (lane 3), indicating that Rabep1 bridges an interaction between PC1 and GGA1. Our data provide evidence that GGA1 is recruited to the polycystin complex by Rabep1 and plays a critical role for subsequent ciliary targeting from the TGN.

GGA proteins are recruited to the TGN membrane *via* their direct interaction with specific Arf members[43, 46]. Since GGA1 effected by the known Arfs such as Arf1[47] or Arf3[42] has not been shown to be involved in ciliary trafficking, we reasoned that additional small GTPases would likely be required to confer specificity of polycystin complex ciliary targeting. A previous study using a small CD16.7-PC1 chimeric construct encoding the last 112 amino acids of the PC1 cytoplasmic C-terminus[29] has implicated Arf4[48] in the ciliary trafficking of PC1. We have asked whether Arf4 may cooperate with GGA1 at the polycystin complex. However we were unable to detect Arf4 in the PC1- complex from the CD cell lysates (Fig. 6c). Arl3, a closely related member of the Arf family, localizes to the Golgi membrane and other microtubule-related structures including cilia[49, 50]. Remarkably,

Arl3 inactivation in mice results in cystic kidney disease[51], reminiscent to what is found in *Pkd1*$^{V/V}$ mice lacking PC1 GPS cleavage[15]. We thus hypothesized that Arl3 binds GGA1 on polycystin complex to regulate its ciliary targeting. Indeed, PC1 co-immunoprecipitated both Arl3 and GGA1, along with Rabep1 and PC2 (Fig. 7a, b). Importantly, Arl3 knockdown in CD cells abolished the ciliary localization of PC1 and PC2 (Fig. 7d, e), indicating a critical role of Arl3 for the ciliary targeting of the polycystin complex.

We then analyzed mutual requirements of Arl3, GGA1 and Rabep1 for PC1 binding. Rabep1 knockdown disrupted the interaction of PC1 with both GGA1 and Arl3 (Fig. 7f, lane 2), whereas the PC1-Rabep1 interaction still occurred when GGA1 or Arl3 was knocked down (lane 3 or 4). Arl3 knockdown however did not disrupt the interaction of PC1 with Rabep1 or GGA1 (lane 4). These results raised the possibility that Rabep1 may recruit a GGA1/Arl3 complex to the polycystin complex by interacting with GGA1. In support of this notion, we found that endogenous GGA1 and Arl3 can be co-immunoprecipitated from CD cells depleted of Rabep1 (Fig. 7g) or in *Pkd1*$^{-/-}$ MEFs (Fig. 7h). Furthermore, when retained in a pre-Golgi compartment in *Pkd2*$^{-/-}$ MEFs, PC1-Rabep1 complex did not bind GGA1 or Arl3 (Fig. 7c). Collectively, our data support a model in which Rabep1 recruits the polycystin complex to GGA1/Arl3 at TGN for ciliary trafficking.

DISCUSSION

To study ciliary membrane protein trafficking, we focused on two large transmembrane proteins, PC1 and PC2, the products of the genes mutated in human autosomal dominant polycystic kidney disease. Our study shows that polycystin trafficking to the cilium occurs in a two-step process. First, PC1 and PC2 must interact and form a complex to traffic from the ER to the Golgi. In addition, PC1 must be cleaved at GPS for this to occur. Rabep1 binds the polycystin complex at PC1's C-terminal tail and rides on the complex to the Golgi but is not itself required for this step in trafficking. Second, once the polycystin complex-bound Rabep1 reaches the TGN, it binds GGA1 that is associated with Arl3 for subsequent targeting to the cilium.

Our finding that a direct PC1-PC2 interaction is required for ciliary trafficking is consistent with some[2, 25], but differs from other published studies[28, 30]. Some of the discrepant findings may be due to the use of overexpression systems by several authors while we have focused on analyzing trafficking of endogenous proteins. It has been previously proposed that PC2 is continuously released from the ER to the Golgi in a COPII-dependent fashion but immediately returned *via* an ER retention/retrieval signal in the C-terminus[20, 30, 52]. A more recent study reported that a small portion of PC2 escapes retrograde transport and traffics to the cilium directly from the *cis*-Golgi compartment without traversing the Golgi apparatus[30]. This was inferred in part from the complete EndoH sensitivity of PC2 at the whole-cell lysate level. We used co-immunoprecipitation to isolate the fraction of PC2 that is complexed with PC1 from native tissue and cell lysates and found that a significant portion was EndoH-resistant ($PC2_{130}$). $PC2_{130}$ is present in a rather small fraction of the total cellular PC2 and has not been recognized previously when analyzed at whole-cell lysate levels, probably because it is obscured by the much more abundant EndoH-sensitive ER-resident $PC2_{120}$ that migrates at a very close position on Western blots. Our co-

immunoprecipitation strategy simultaneously enriches the native polycystin complex and removes the predominant interfering EndoH-sensitive $PC2_{120}$ form that is not complexed with PC1, thereby allowing the visualization of $PC2_{130}$ of the polycystin complex. Our finding of exclusive EndoH-resistance of both PC1 and PC2 in isolated cilia provided direct biochemical evidence that the polycystin complex traffics to cilia in fact through the Golgi apparatus. The ciliary polycystins may represent some of the EndoH-resistant polycystin complex population detected in native kidney tissues and cells. But given the relatively small volume occupied by the cilium, most of this polycystin population probably resides on non-ciliary compartments such as the Golgi or post-Golgi vesicles, or at the plasma membrane[18]. Further studies are required to resolve this issue.

PC1 is generally far less abundant than PC2 in kidneys and is the central determinant of cyst formation in polycystic kidney and liver diseases[53, 54]. We find that ectopic expression of PC1 can induce the ER-resident endogenous PC2 to translocate to the cilium. This data supports the idea that PC1 is the rate-limiting factor for ciliary trafficking of the polycystin complex in renal epithelial cells. We propose that the PC1-PC2 interaction is required to counteract and overcome the retrograde transport of the polycystin complex to the ER by masking the ER retention/retrieval signals or alternatively by allowing the complex to pass quality-control checkpoints in the ER as found for many GPCRs[55]. This allows the complex to efficiently reach the TGN for subsequent ciliary targeting by a Rabep1/GGA1/Arl3-dependent process.

GPS cleavage of PC1 also is required for the polycystin complex to move to the TGN. None the less, the non-cleavable $PC1^{V}$ can still move to the Golgi apparatus as evidenced by its ability of acquiring EndoH-resistance ($PC1^{V\text{-}600}$, Fig. 5d, e). One possible explanation is that $PC1^{V}$ cannot remain associated with PC2 at the Golgi apparatus and consequently traffics to a non-ciliary location yet to be determined. Cleavage may promote the trafficking of the polycystin complex to the Golgi apparatus by increasing PC1/PC2 binding affinity, thereby inhibiting PC2 dissociation. Alternatively, cleavage could increase the ER-to-Golgi transition rate of the polycystin complex, thereby outpacing PC2 dissociation. GPS cleavage could be significant for regulating polycystin trafficking in the kidney in a development-specific manner. In early embryonic stages, PC1 exists largely in its uncleaved form and therefore it might mainly traffic, perhaps apart from PC2, to a non-ciliary location such as at the cell-cell junction where it could regulate convergent extension and elongation of developing renal tubules[17, 56]. After birth, however, PC1 is mostly cleaved[15, 17, 18] and probably traffics to the cilia in the form of the polycystin complex to control proper tubular diameter[56].

Previous efforts have focused on the identification of the ciliary targeting motifs and binding proteins that may mediate ciliary trafficking[57]. Both PC1 and PC2 have been reported to contain ciliary-targeting signals. For PC1 the sequence is at its extreme C-terminus[29], while for PC2 the ciliary targeting sequence is within the first 15 amino acids at the N-terminus[28]. Our findings indicate that the ciliary targeting signal in each polycystin is not sufficient for ciliary trafficking in renal epithelial cells. We have identified a novel ciliary sorting module that is composed of Rabep1, GGA1 and Arl3, which is recruited to the polycystin complex by PC1 and is required for the ciliary targeting of the complex. Rabep1-PC1 binding

requires the intact coiled-coil domain of PC1, which is outside of the previously reported ciliary targeting sequence[29]. The same study using a small CD16.7-PC1 chimeric construct encoding the last 112 amino acids of the PC1 cytoplasmic C-terminus[29] has also implicated Arf4 in the ciliary trafficking of PC1. However we were unable to detect Arf4-binding to full-length endogenous PC1 in CD cells, which makes it unlikely that Arf4 plays an important role in targeting of the polycystin complex.

GGA1 is a member of the monomeric GGA family that is known to select proteins at the TGN into clathrin- and GGA-coated carriers, which are then transported to endosomes. GGA1 exerts its function by the different domains that interact with various other proteins[44]. The GAT domain binds activated Arf-family GTP-binding proteins and thereby recruits GGA1 to the TGN. The hinge domain then binds clathrin for vesicle budding, while the GAE domain binds accessory factors that can regulate the function of GGA-coated carriers. Arl3 plays a critical role in ciliary function and is involved in intraflagellar transport in *C. elegans*[58]. In mice, *Arl3* in activation results in various ciliopathy-related phenotypes including cystic kidney disease and retinal degeneration[51]. In addition to the cilium, Arl3 also has been shown to localize to the Golgi but the function of this Golgi-associated pool is unknown[50]. We show for the first time that there is a distinct pool of Arl3 that is bound to GGA1. This GGA1/Arl3 module likely binds cargo and other components necessary for clathrin binding, forming vesicle carriers destined for the cilium. Since Arl3 is known to have microtubule-binding activity[50], one possibility is that Arl3 may direct the cargo-bearing vesicles to cytoplasmic microtubules for dynein-driven transport to the cilium. The dynein-dependent system has been reported to translocate rhodopsin-bearing vesicles along microtubules towards the cilium in polarized epithelia[59].

A central region of Rabep1 has been shown to interact with the GAE domain of GGA1[45]. The Rabep1-GGA1 interaction is bipartite, as the C-terminal coiled-coil region of Rabep1 also binds the GAT domain of GGA1. This bivalent interaction is thought to mediate fusion of post-Golgi GGA1-coated vesicles to Rabep1-bearing endosomes. PC1 binds the C-terminal coiled-coil region of Rabep1 that usually binds to GAT, thus likely leaving its central region accessible for interacting with the GAE domain of GGA1/Arl3. Our current model is that polycystin complex-bound Rabep1 serves as an accessory protein for GGA1 *via* its GAE domain, thereby coupling the polycystin complex to the GGA1/Arl3 module (Fig.8). It remains to be determined whether this module may be involved in the later stages of ciliary trafficking as recently described for Rabep1[60] and Arl3[61, 62]. Further studies are also required to investigate how the Rabep1/GGA1/Arl3 complex is related to the previously identified trafficking complexes including the exocyst[63] and BBSome[64].

Our model has several important implications. First, this general mechanism could conceivably be used to transport the polycystin complex to other cellular locations. For example, the Rabep1-GGA1-polycystin complex could bind other members of the ARF family. This may result in trafficking to non-ciliary locations such as the plasma membrane where polycystins have also been detected[25, 26, 27]. Second, since the interactions between Rabep1, GGA1 and Arl3 can occur independently of PC1, Rabep1 may bind and couple other ciliary membrane proteins to the GGA1/Arl3 module for ciliary targeting. Third, because the interaction between GGA1 and Arl3 can occur independently Rabep1, one can

imagine that accessory proteins other than Rabep1 may bind and couple yet other ciliary membrane proteins to GGA1/Arl3 *via* the GAE domain for ciliary targeting. In summary, this work provides novel insights into the mechanism of the ciliary trafficking of membrane proteins.

METHODS

Cell lines

Collecting duct (CD) cells were affinity-purified from mouse postnatal kidneys by using DBA-conjugated Dynabeads (Invitrogen). The kidneys were minced into small pieces and digested in MEM/F12 containing 0.2% collagenase, 0.2% hyaluronidase, and 0.001% DNase I at 37°C for 2 h with gentle agitation. The digested tissue was incubated with Dynabeads at 4°C for 30 min. The cells bound to the beads were suspended in culture medium for propagation[15]. Tetracycline-inducible and stable MDCK and IMCD cells were generated using Flp-In^{TM} System (Invitrogen)[65, 66] by transfecting pcDNA5-based wild-type or mutant *Pkd1* expression plasmids according to the manufacturer's protocol. MDCK cell lines were cultured in DMEM growth media with 100μgml^{-1}hygromycin B and 5μgml^{-1}blasticidin. Stable IMCD cell lines were cultured in DMEM/F12 growth media with 50 μgml^{-1}hygromycin B.

Cilia preparation

MDCK cells were cultured on Transwell filter for ~10 days for cilium growth using DMEM with 10% FBS at the outside membrane and DMEM without FBS at the inside membrane of transwell plate. The cells were washed with PBS and treated with 30 mM ammonium sulfate for 3 h to shed cilia into the medium[36]. Intact shed cilia were collected from the medium by sequential centrifugation (at 2,000 × g for 30 min, 10,000 × g for 30 min, and at 16,000 × g for 30 min). After centrifugation, the cilia pellet was resuspended in PBS for immunofluorescence or Western blot analysis.

Immunofluorescence

Cultured cells were fixed in 4% formaldehyde for 15 min and then permeabilized by 0.1% Triton X-100 for 5 min, and incubated with primary antibodies in blocking buffer (5% FBS/ 0.05% Triton X-100 in PBS) for overnight. Cells were then incubated with fluorescence conjugated secondary antibodies (Invitrogen, CA) for 1 h and mounted by Vecta Shield Mountaing Medium (Vector Laboratories, CA). Confocal microscope LSM 510 (Carl Zeiss Microscopy) was used to acquire images. For paraffin embedded kidney sections, sections were first deparaffinized by xylene for 10 min and rehydrated using a graded series of alcohol solutions, followed by antigen retrieval using Target Retrieval Solution, Citrate Buffer pH 6 (Dako, CA), and then followed the procedure as previously described[15]. The primary antibodies used for immunofluorescence included mouse anti-acetylated tubulin from Sigma-Aldrich (T7451, 1:4,000) and rabbit anti-Arl13b from Protein tech (17711–1-AP, 1:200) for cilia markers, and rabbit anti-PC2[34](1:200).

Immunoprecipitation and immunoblot analysis

Immunoprecipitation (IP) studies of the endogenous and recombinant PC1 were accomplished on mouse tissue samples and cells (MEFs, collecting duct cells, MDCK) homogenized in lysis buffer(20 mM sodium phosphate, pH 7.2/150 mM NaCl/1 mM EDTA/10% (vol/vol) glycerol/1% Triton X-100/protease inhibitors)[15]. Briefly, the homogenate was incubated with primary antibody or antibody-conjugated bead for overnight, followed by incubation with G Sepharose^{TM} 4 Fast Flow (GE Healthcare) or goat anti-chicken IgY agarose beads (Precip Hen, Aves) for 3 h. Bead pellets were washed with lysis buffer three times and eluded with SDS sample buffer. The primary antibodies and antibody conjugated bead used for IP included mouse anti-FLAG M2 affinity gel from Sigma-Aldrich (A2220), rabbit anti-FLAG from Cell Signaling Technology (#2368, 1:50), chicken anti-PC1 (α-CC, 1–2 μgml^{-1})[15], rabbit anti-Myc from Cell Signaling Technology (#2278, 1:200), and rabbit anti-GGA1 from Thermo Scientific (PA5–12130, 1–2 μgml^{-1}). The protein samples were loaded on 3–8% Tris-Acetate SDS-polyacrylamide precast gels or 4–12% Tris-Glycine SDS-polyacrylamide precast gels (Invitrogen) and transferred to PVDF membrane (Bio-Rad). The membranes were incubated with primary antibodies for overnight and then washed with TBS-Tween 20 buffer. An HRP-conjugated secondary antibody from GE Healthcare (NA934V; 1:10,000) was incubated for 1 h and then ECL Prime (GE Healthcare) was used for detection on a Kodak film. The membranes were then stripped using Restore Western blot buffer (Pierce, VWR) and reprobed. The primary antibodies used for immunoblotting included mouse anti-PC1 (7e12) from Santa Cruz Biotechnology (sc-130554, 1:1,000), mouse anti-β-actin from Sigma-Aldrich (A5316, 1:10,000), rabbit anti-Polaris from Thermo Scientific (PA5–18467, 1:1,000), mouse anti-Alix from Cell Signaling Technology (#2171, 1:1,000), mouse anti-Rabep1 from BD Bioscience (610676, 1:1,000), rabbit anti-GGA1 from Abcam (ab38454, 1:500), rabbit anti-c-MET from Cell Signaling Technology (#8198, 1:1,000), rabbit anti-IGFBP-2 (11065–3-AP, 1:1000), rabbit anti-Arf4 (11673–1-AP, 1:1,000), and rabbit anti-Arl3 (10961–1-AP, 1:500)from Protein tech. E4 monoclonal antibody against PC1 was generated from mice immunized with recombinant 130 aa polypeptide corresponding to residues 406–535 (C-lectin binding domain) of human PC1 protein. The specificity is shown in Supplementary Fig. 5.

N-glycosylation analysis

Immunoprecipitation products or lysates were denatured using glycoprotein denature buffer (New England Biolabs) for 1 min at 95 °C and then quickly chilled on ice. The denatured glycoprotein was incubated with PNGaseF or EndoH (New England Biolabs) for 1 h at 37°C.

shRNA sequences and lentiviral infection

pGIPZ Lentiviral shRNAs (Thermo Scientific) were used to inhibit the expression of target genes. For PC1 knockdown, we used three pGIPZ Lentiviral shRNAs containing following antisense sequences: *Pkd1* antisense #1;5′-AAGCCAATGAGGTCACCAG-3′, *Pkd1* antisense #2;5′-AACGCAGCAGTAATCTGCT-3′, and *Pkd1* antisense#3;5′-TTCTCTCCAGGAACACTGG-3′. We have also constructed pGIPZ Lentiviral shRNA inserted with previously reported si*Pkd1*^{3297} sequences 5′-

CATGTGAGCAACATCACC-3′[67] using *Xho*I and *Mlu*I. These *Pkd1* shRNAs showed up to ~90% knockdown of PC1 (Supplementary Fig. 2a, b). For PC2 knockdown, we used pGIPZ Lentivirals hRNA containing following antisense sequences 5′-TTTCCAATATCTCTTCCAC-3′. For Rabep1, GGA1, and Arl3 inhibition, we used three shRNAs for Rabep1, four shRNAs for GGA1, and two shRNAs for Arl3. Rabep1 antisense #1;5′-TAAATTCTTGCTCAAGCTG-3′, Rabep1 antisense #2;5′-TCATCTATAGCTTCTTGCT-3′, Rabep1 antisense #3;5′-TGTTGTTCATCCTCCTCCT-3′, GGA1 antisense #1;5′-TTGATGAGCTTATTGGCAG-3′, GGA1 antisense #2;5′-TGTACAGGTTGATCACCTG-3′, GGA1 antisense #3;5′-ACAGGTTGATCACCTGGGT-3′, GGA1 antisense #4;5′-TCAGCTCTGTGACCACAGG-3′, Arl3 antisense #1;5′-TTCTTCCTCCAGTAATTCC-3′, Arl3 antisense #2;5′-AACTTCTCCAGTATGGTCT-3′.pGIPZ Lentiviral vector containing gene specific shRNA was transfected into 293T cells with viral packaging plasmids and the resulting lentivirus were produced and used according to the manufacture's instruction.

Yeast two-hybrid screening

The human PKD1 cDNA (Accession L33243) fragment corresponding to bp12,473–13,120 encoding the C-terminal 215 amino acids was isolated by PCR and subcloned into the *Sal*I and *Not*I sites of the pPC97 vector in-frame with the GAL4 DNA-binding domain[68]. YRG-2 yeast cells (Stratagene) were transformed with bait and subsequently with an adult rat hippocampus random primed cDNA library cloned into pPC86. The protocols used in this yeast two-hybrid system were performed as described previously[22]. Briefly, positive yeast clones were selected on triple-deficient plates (Leu-, Trp-, and His) and confirmed by positive β-gal activity. The pPC86-based prey plasmids were recovered and co-transformed into YRG-2 with either the bait vector or the original pPC97 vector to confirm the interaction.

Statistical analysis

Statistical analysis was performed by ANOVA to calculate statistical significance between more than two experimental groups. Student's t-test was used for the statistical significance between two experimental groups. All data are presented as mean ± SEM.

Supplementary Material

Refer to Web version on PubMed Central for supplementary material.

Acknowledgments

The authors are thankful to Dr. Owen Woodward for reading and commenting on the manuscript. This work was supported by grants from the National Institutes of Health R01 DK062199, National Kidney Foundation of Maryland to F.Q., the Korea Research Foundation Grant funded by the Korean Government (KRF-2008–357-E00030), the National Kidney Foundation of Maryland to H.K., R01DK076017, R01DKDK095036 to T.W., R37DK48006 and the NIDDK Intramural Program 1ZIADK075042 to G.G.G., and DK55881 and the Research Service, Department of Veterans Affairs to E.J.W. These studies utilized resources provided by the NIDDK sponsored Baltimore Polycystic Kidney Disease Research and Clinical Core Center, P30DK090868. We thank members of the Baltimore PKD Center for insightful discussions.

References

1. Singla V, Reiter JF. The primary cilium as the cell's antenna: signaling at a sensory organelle. Science. 2006; 313:629–633. [PubMed: 16888132]
2. Nauli SM, et al. Polycystins 1 and 2 mediate mechanosensation in the primary cilium of kidney cells. Nat Genet. 2003; 33:129–137. [PubMed: 12514735]
3. Pazour GJ. Intraflagellar transport and cilia-dependent renal disease: the ciliary hypothesis of polycystic kidney disease. J Am Soc Nephrol. 2004; 15:2528–2536. [PubMed: 15466257]
4. Hu Q, et al. A septin diffusion barrier at the base of the primary cilium maintains ciliary membrane protein distribution. Science. 2010; 329:436–439. [PubMed: 20558667]
5. Nachury MV, Seeley ES, Jin H. Trafficking to the ciliary membrane: how to get across the periciliary diffusion barrier? Annual review of cell and developmental biology. 2010; 26:59–87.
6. Pedersen LB, Rosenbaum JL. Intraflagellar transport (IFT) role in ciliary assembly, resorption and signalling. Current topics in developmental biology. 2008; 85:23–61. [PubMed: 19147001]
7. Consortium TEPKD. The polycystic kidney disease 1 gene encodes a 14 kb transcript and lies within a duplicated region on chromosome 16. Cell. 1994; 77:881–894. [PubMed: 8004675]
8. Mochizuki T, et al. PKD2, a gene for polycystic kidney disease that encodes an integral membrane protein. Science. 1996; 272:1339–1342. [PubMed: 8650545]
9. Pazour GJ, San Agustin JT, Follit JA, Rosenbaum JL, Witman GB. Polycystin-2 localizes to kidney cilia and the ciliary level is elevated in orpk mice with polycystic kidney disease. Current biology : CB. 2002; 12:R378–380. [PubMed: 12062067]
10. Yoder BK, Hou X, Guay-Woodford LM. The polycystic kidney disease proteins, polycystin-1, polycystin-2, polaris, and cystin, are co-localized in renal cilia. J Am Soc Nephrol. 2002; 13:2508–2516. [PubMed: 12239239]
11. Praetorius HA, Spring KR. Bending the MDCK cell primary cilium increases intracellular calcium. The Journal of membrane biology. 2001; 184:71–79. [PubMed: 11687880]
12. Hughes J, et al. The polycystic kidney disease 1 (PKD1) gene encodes a novel protein with multiple cell recognition domains. Nat Genet. 1995; 10:151–160. [PubMed: 7663510]
13. Nims N, Vassmer D, Maser RL. Transmembrane domain analysis of polycystin-1, the product of the polycystic kidney disease-1 (PKD1) gene: evidence for 11 membrane-spanning domains. Biochemistry. 2003; 42:13035–13048. [PubMed: 14596619]
14. Qian F, et al. Cleavage of polycystin-1 requires the receptor for egg jelly domain and is disrupted by human autosomal-dominant polycystic kidney disease 1-associated mutations. Proc Natl Acad Sci U S A. 2002; 99:16981–16986. [PubMed: 12482949]
15. Yu S, et al. Essential role of cleavage of Polycystin-1 at G protein-coupled receptor proteolytic site for kidney tubular structure. Proc Natl Acad Sci U S A. 2007; 104:18688–18693. [PubMed: 18003909]
16. Wei W, Hackmann K, Xu H, Germino G, Qian F. Characterization of cis-autoproteolysis of polycystin-1, the product of human polycystic kidney disease 1 gene. J Biol Chem. 2007; 282:21729–21737. [PubMed: 17525154]
17. Castelli M, et al. Polycystin-1 binds Par3/aPKC and controls convergent extension during renal tubular morphogenesis. Nature communications. 2013; 4:2658.
18. Kurbegovic A, et al. Novel functional complexity of polycystin-1 by GPS cleavage in vivo: role in polycystic kidney disease. Molecular and cellular biology. 2014; 34:3341–3353. [PubMed: 24958103]
19. Arac D, et al. A novel evolutionarily conserved domain of cell-adhesion GPCRs mediates autoproteolysis. The EMBO journal. 2012; 31:1364–1378. [PubMed: 22333914]
20. Cai Y, et al. Identification and characterization of polycystin-2, the PKD2 gene product. J Biol Chem. 1999; 274:28557–28565. [PubMed: 10497221]
21. Koulen P, et al. Polycystin-2 is an intracellular calcium release channel. Nat Cell Biol. 2002; 4:191– 197. [PubMed: 11854751]
22. Qian F, Germino FJ, Cai Y, Zhang X, Somlo S, Germino GG. PKD1 interacts with PKD2 through a probable coiled-coil domain. Nat Genet. 1997; 16:179–183. [PubMed: 9171830]

23. Tsiokas L, Kim E, Arnould T, Sukhatme VP, Walz G. Homo- and heterodimeric interactions between the gene products of PKD1 and PKD2. Proc Natl Acad Sci U S A. 1997; 94:6965–6970. [PubMed: 9192675]
24. Zhu J, et al. Structural model of the TRPP2/PKD1 C-terminal coiled-coil complex produced by a combined computational and experimental approach. Proc Natl Acad Sci U S A. 2011; 108:10133–10138. [PubMed: 21642537]
25. Chapin HC, Rajendran V, Caplan MJ. Polycystin-1 surface localization is stimulated by polycystin-2 and cleavage at the G protein-coupled receptor proteolytic site. Mol Biol Cell. 2010; 21:4338–4348. [PubMed: 20980620]
26. Grimm DH, et al. Polycystin-1 distribution is modulated by polycystin-2 expression in mammalian cells. J Biol Chem. 2003; 278:36786–36793. [PubMed: 12840011]
27. Hanaoka K, et al. Co-assembly of polycystin-1 and-2 produces unique cation-permeable currents. Nature. 2000; 408:990–994. [PubMed: 11140688]
28. Geng L, et al. Polycystin-2 traffics to cilia independently of polycystin-1 by using an N- terminal RVxP motif. Journal of cell science. 2006; 119:1383–1395. [PubMed: 16537653]
29. Ward HH, et al. A conserved signal and GTPase complex are required for the ciliary transport of polycystin-1. Mol Biol Cell. 2011; 22:3289–3305. [PubMed: 21775626]
30. Hoffmeister H, et al. Polycystin-2 takes different routes to the somatic and ciliary plasma membrane. J Cell Biol. 2011; 192:631–645. [PubMed: 21321097]
31. Xu C, et al. Human ADPKD primary cyst epithelial cells with a novel, single codon deletion in the PKD1 gene exhibit defective ciliary polycystin localization and loss of flow-induced Ca2+ signaling. Am J Physiol Renal Physiol. 2007; 292:F930–945. [PubMed: 17090781]
32. Freedman BS, et al. Reduced ciliary polycystin-2 in induced pluripotent stem cells from polycystic kidney disease patients with PKD1 mutations. J Am Soc Nephrol. 2013; 24:1571–1586. [PubMed: 24009235]
33. Piontek K, Menezes LF, Garcia-Gonzalez MA, Huso DL, Germino GG. A critical developmental switch defines the kinetics of kidney cyst formation after loss of Pkd1. Nat Med. 2007; 13:1490–1495. [PubMed: 17965720]
34. Cebotaru V, et al. Polycystin-1 negatively regulates Polycystin-2 expression via the aggresome/autophagosome pathway. J Biol Chem. 2014; 289:6404–6414. [PubMed: 24459142]
35. Freeze, HH. Use of glycosidases to study protein trafficking. In: Bonifacino, Juan S., et al., editors. Current protocols in cell biology/editorial board. Vol. Chapter 15. 2001. p. 12
36. Overgaard CE, Sanzone KM, Spiczka KS, Sheff DR, Sandra A, Yeaman C. Deciliation is associated with dramatic remodeling of epithelial cell junctions and surface domains. Mol Biol Cell. 2009; 20:102–113. [PubMed: 19005211]
37. Pisitkun T, Shen RF, Knepper MA. Identification and proteomic profiling of exosomes in human urine. Proc Natl Acad Sci U S A. 2004; 101:13368–13373. [PubMed: 15326289]
38. Webb CP, Lane K, Dawson AP, Vande Woude GF, Warn RM. C-Met signalling in an HGF/SF-insensitive variant MDCK cell line with constitutive motile/invasive behaviour. Journal of cell science. 1996; 109 (Pt 9):2371–2381. [PubMed: 8886986]
39. Shalamanova L, Kubler B, Scharf JG, Braulke T. MDCK cells secrete neutral proteases cleaving insulin-like growth factor-binding protein-2 to-6. American journal of physiology Endocrinology and metabolism. 2001; 281:E1221–1229. [PubMed: 11701437]
40. Stenmark H, Vitale G, Ullrich O, Zerial M. Rabaptin-5 is a direct effector of the small GTPase Rab5 in endocytic membrane fusion. Cell. 1995; 83:423–432. [PubMed: 8521472]
41. Wodarczyk C, Rowe I, Chiaravalli M, Pema M, Qian F, Boletta A. A novel mouse model reveals that polycystin-1 deficiency in ependyma and choroid plexus results in dysfunctional cilia and hydrocephalus. PLoS One. 2009; 4:e7137. [PubMed: 19774080]
42. Boman AL, Zhang C, Zhu X, Kahn RA. A family of ADP-ribosylation factor effectors that can alter membrane transport through the trans-Golgi. Mol Biol Cell. 2000; 11:1241–1255. [PubMed: 10749927]
43. Bonifacino JS. The GGA proteins: adaptors on the move. Nat Rev Mol Cell Biol. 2004; 5:23–32. [PubMed: 14708007]

44. Puertollano R, Randazzo PA, Presley JF, Hartnell LM, Bonifacino JS. The GGAs promote ARF-dependent recruitment of clathrin to the TGN. Cell. 2001; 105:93–102. [PubMed: 11301005]
45. Mattera R, Arighi CN, Lodge R, Zerial M, Bonifacino JS. Divalent interaction of the GGAs with the Rabaptin-5-Rabex-5 complex. The EMBO journal. 2003; 22:78–88. [PubMed: 12505986]
46. Kahn RA, et al. Arf family GTPases: roles in membrane traffic and microtubule dynamics. Biochem Soc Trans. 2005; 33:1269–1272. [PubMed: 16246095]
47. Dell' Angelica EC, et al. GGAs: a family of ADP ribosylation factor-binding proteins related to adaptors and associated with the Golgi complex. J Cell Biol. 2000; 149:81–94. [PubMed: 10747089]
48. Wang J, Deretic D. Molecular complexes that direct rhodopsin transport to primary cilia. Progress in retinal and eye research. 2014; 38:1–19. [PubMed: 24135424]
49. Van Valkenburgh H, Shern JF, Sharer JD, Zhu X, Kahn RA. ADP-ribosylation factors (ARFs) and ARF-like 1 (ARL1) have both specific and shared effectors: characterizing ARL1-binding proteins. J Biol Chem. 2001; 276:22826–22837. [PubMed: 11303027]
50. Zhou C, Cunningham L, Marcus AI, Li Y, Kahn RA. Arl2 and Arl3 regulate different microtubule-dependent processes. Mol Biol Cell. 2006; 17:2476–2487. [PubMed: 16525022]
51. Schrick JJ, Vogel P, Abuin A, Hampton B, Rice DS. ADP-ribosylation factor-like 3 is involved in kidney and photoreceptor development. The American journal of pathology. 2006; 168:1288–1298. [PubMed: 16565502]
52. Kottgen M, et al. Trafficking of TRPP2 by PACS proteins represents a novel mechanism of ion channel regulation. The EMBO journal. 2005; 24:705–716. [PubMed: 15692563]
53. Fedeles SV, et al. A genetic interaction network of five genes for human polycystic kidney and liver diseases defines polycystin-1 as the central determinant of cyst formation. Nat Genet. 2011; 43:639–647. [PubMed: 21685914]
54. Hopp K, et al. Functional polycystin-1 dosage governs autosomal dominant polycystic kidney disease severity. J Clin Invest. 2012; 122:4257–4273. [PubMed: 23064367]
55. Margeta-Mitrovic M, Jan YN, Jan LY. A trafficking checkpoint controls GABA(B) receptor heterodimerization. Neuron. 2000; 27:97–106. [PubMed: 10939334]
56. Karner CM, Chirumamilla R, Aoki S, Igarashi P, Wallingford JB, Carroll TJ. Wnt9b signaling regulates planar cell polarity and kidney tubule morphogenesis. Nat Genet. 2009; 41:793–799. [PubMed: 19543268]
57. Emmer BT, Maric D, Engman DM. Molecular mechanisms of protein and lipid targeting to ciliary membranes. Journal of cell science. 2010; 123:529–536. [PubMed: 20145001]
58. Li Y, Wei Q, Zhang Y, Ling K, Hu J. The small GTPases ARL-13 and ARL-3 coordinate intraflagellar transport and ciliogenesis. J Cell Biol. 2010; 189:1039–1051. [PubMed: 20530210]
59. Tai AW, Chuang JZ, Bode C, Wolfrum U, Sung CH. Rhodopsin's carboxy-terminal cytoplasmic tail acts as a membrane receptor for cytoplasmic dynein by binding to the dynein light chain Tctex-1. Cell. 1999; 97:877–887. [PubMed: 10399916]
60. Omori Y, et al. Elipsa is an early determinant of ciliogenesis that links the IFT particle to membrane-associated small GTPase Rab8. Nat Cell Biol. 2008; 10:437–444. [PubMed: 18364699]
61. Ismail SA, Chen YX, Miertzschke M, Vetter IR, Koerner C, Wittinghofer A. Structural basis for Arl3-specific release of myristoylated ciliary cargo from UNC119. The EMBO journal. 2012; 31:4085–4094. [PubMed: 22960633]
62. Wright KJ, et al. An ARL3-UNC119-RP2 GTPase cycle targets myristoylated NPHP3 to the primary cilium. Genes & development. 2011; 25:2347–2360. [PubMed: 22085962]
63. Fogelgren B, et al. The exocyst protein Sec10 interacts with Polycystin-2 and knockdown causes PKD-phenotypes. PLoS genetics. 2011; 7:e1001361. [PubMed: 21490950]
64. Su X, et al. Bardet-Biedl syndrome proteins 1 and 3 regulate the ciliary trafficking of polycystic kidney disease 1 protein. Hum Mol Genet. 2014; 23:5441–5451. [PubMed: 24939912]
65. Sang L, et al. Mapping the NPHP-JBTS-MKS protein network reveals ciliopathy disease genes and pathways. Cell. 2011; 145:513–528. [PubMed: 21565611]

66. Woodward OM, et al. Identification of a polycystin-1 cleavage product, P100, that regulates store operated Ca entry through interactions with STIM1. PLoS One. 2010; 5:e12305. [PubMed: 20808796]

67. Battini L, et al. Loss of polycystin-1 causes centrosome amplification and genomic instability. Hum Mol Genet. 2008; 17:2819–2833. [PubMed: 18566106]

68. Fields S, Sternglanz R. The two-hybrid system: an assay for protein-protein interactions. Trends in genetics : TIG. 1994; 10:286–292. [PubMed: 7940758]

69. Lupas A, Van Dyke M, Stock J. Predicting coiled coils from protein sequences. Science. 1991; 252:1162–1164. [PubMed: 2031185]

70. Qian F, Watnick TJ, Onuchic LF, Germino GG. The molecular basis of focal cyst formation in human autosomal dominant polycystic kidney disease type I. Cell. 1996; 87:979–987. [PubMed: 8978603]

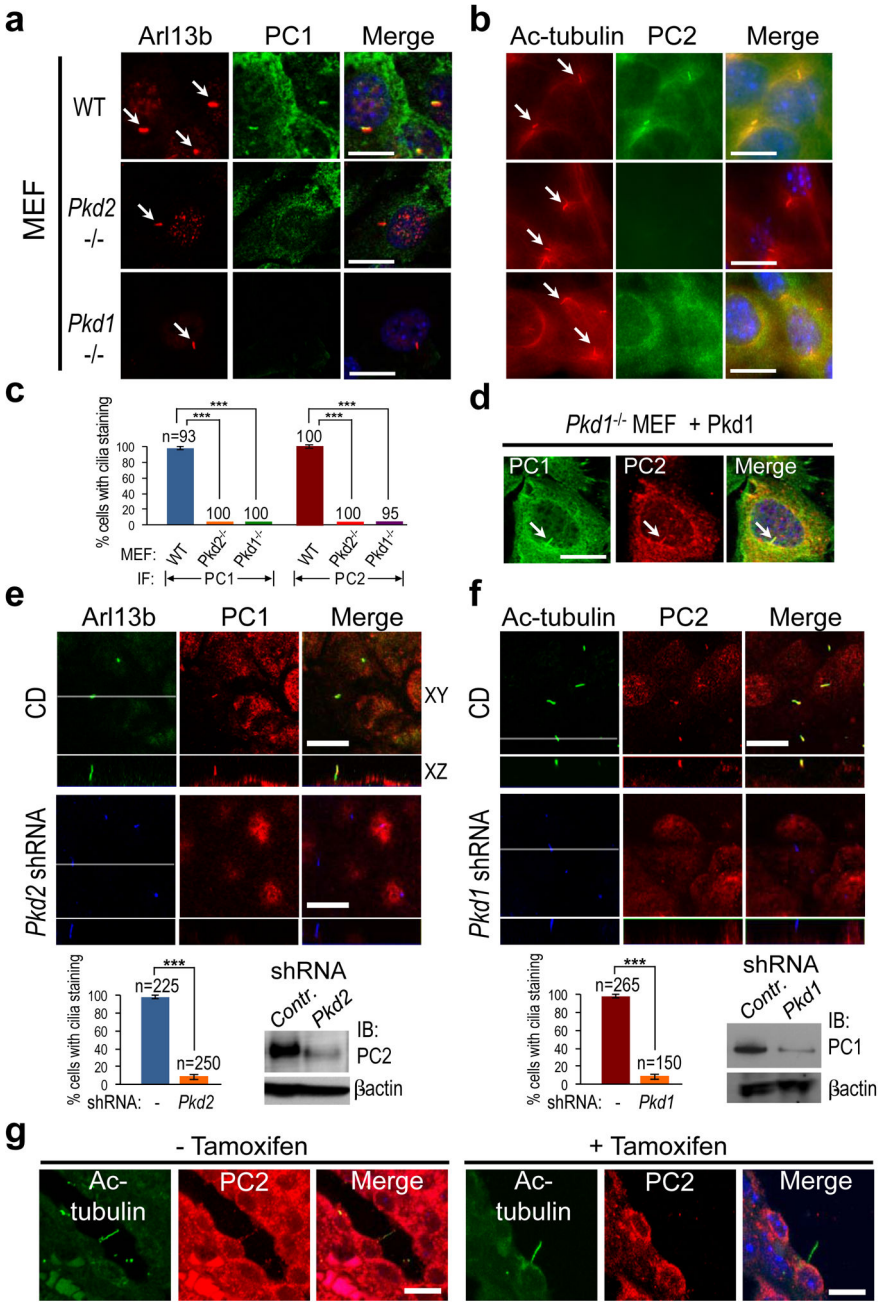

Figure 1.

Native PC1 and PC2 regulate each other's ciliary localization *in vivo*. (**a–b**) Representative immunofluorescence images of MEFs with indicated genotypes subjected to 24_h serum starvation. Cells were stained with anti-PC1 (E4, Supplementary Fig. 5) and analyzed by confocal microscopy (**a**), or stained with anti-PC2 and analyzed by epifluorescence microscopy (**b**). Arl13b or acetylated (Ac)-tubulin was used as a ciliary marker. Arrows indicate cilia. (**c**) The bar diagram shows the quantification of PC1 or PC2 ciliary localization in MEFs with various genotypes with numbers of cells analyzed (n) indicated; *** $p<0.001$. (**d**) Exogenously expressed PC1 traffics to cilia (arrow) and rescues ciliary

localization of PC2 in *Pkd1*$^{-/-}$ MEFs. Exogenous expression of GFP served as a negative control (Supplementary Fig. 1).(**e**) Confocal images of CD cells (upper panel) and CD cells expressing *Pkd2*shRNA (lower panel). Cells were stained with antibodies against Arl13b (blue) and PC1(E4) (red). The bar diagram below shows the quantification of PC1 ciliary localization in CD and cells with *Pkd2* knockdown performed from four independent experiments with numbers of cells analyzed (n) indicated; *** $p<0.001$. Western blot analysis shows that *Pkd2* shRNA reduced endogenous PC2 level by ~90%. (**f**) Confocal images of CD cells (upper panel) and cells expressing *Pkd1*shRNA, stained with antibodies as indicated. Four different *Pkd1* shRNAs had similar results. The bar diagram shows the quantification of PC2 ciliary localization between CD and cells with *Pkd1* knock down from four independent experiments; *** $p<0.001$. Western blot analysis shows that *Pkd1*shRNA reduced endogenous PC1 level by ~90%. The white line in the XY scan in (**e**, **f**) indicates the path of the XZ scan. (**g**) Confocal images of PC2 ciliary localization in collecting duct at P28 in *Pkd1*$^{cko/cko}$:tamoxifen-Cre mouse kidney[33], in which *Pkd1* was not inactivated (left panel, normal tubule) or inactivated by tamoxifen injection on P10 (right panel, cystic tubule). PC2 was detected in 21 of 21 cilia (red) in normal kidneys. Cilia were marked by acetylated tubulin (green). Note that PC2 was not detectable in 18 of 18 cilia of cysts analyzed. Scale bar, 10 μm.

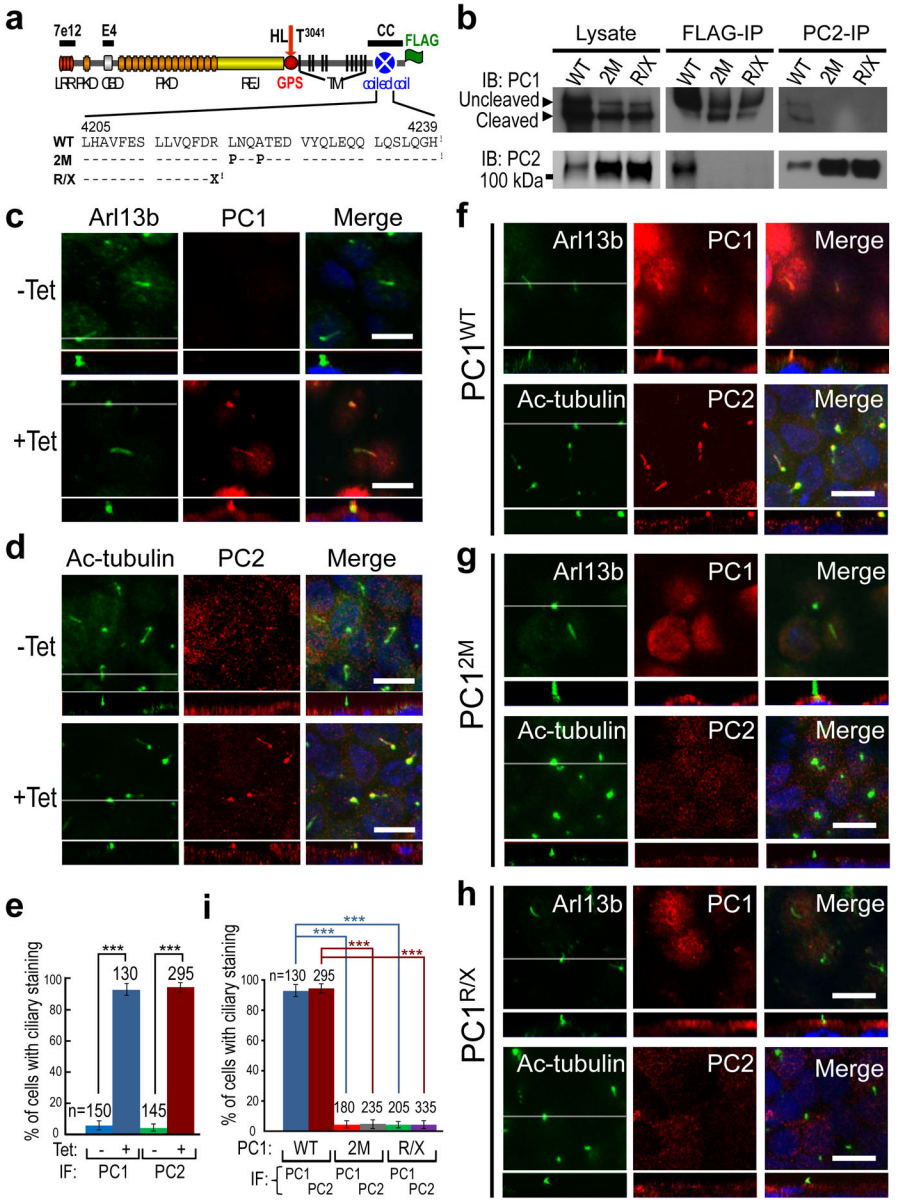

Figure 2.

Direct interaction of PC1 and PC2 is required for ciliary localization.(**a**) A schematic diagram of the domain organization of mouse polycystin-1 with epitope position of antibodies and FLAG-tag indicated. LRR, leucine rich repeat; CLD, C-type lectin binding domain; PKD, polycystic kidney disease repeats; REJ, receptor for egg jelly module; GPS, G-protein-coupled receptor proteolytic site. TM: transmembrane domain. GPS cleavage occurs at HL^T^{3041}. Mutations in the coiled coil domain are indicated below the wild-type (WT) sequence. (**b**) Lysates of the induced MDCK cells were subject to reciprocal immunoprecipitation (IP) with the anti-FLAG or anti-PC2. The IP products were analyzed by Western blotting with antibodies against PC1 (7e12) or PC2 as indicated. (**c, d**) Confocal images of un-induced (-Tet) or induced (+Tet) MDCK^{PC1WT} cells, stained with antibodies

as indicated. The white line in the XY scan indicates the path of the XZ scan. (**e**) Quantification of PC1 and PC2 ciliary localization for (**c,d)** from three independent experiments and presented as the mean ± SEM; *** $p<0.001$. The number of cells analyzed is indicated. (**f**–**h**) Confocal images of induced MDCK cells expressing wild-type or mutant PC1 proteins as indicated, stained with antibodies as indicated. Note that the mutants do not localize to cilia nor induce ciliary localization of endogenous PC2. Scale bar, 10 μm. (**i**) Quantification of PC1 or PC2 ciliary localization in (**f**–**h**) from three independent experiments and presented as the mean ± SEM; *** $p<0.001$. The number of cells analyzed is indicated.

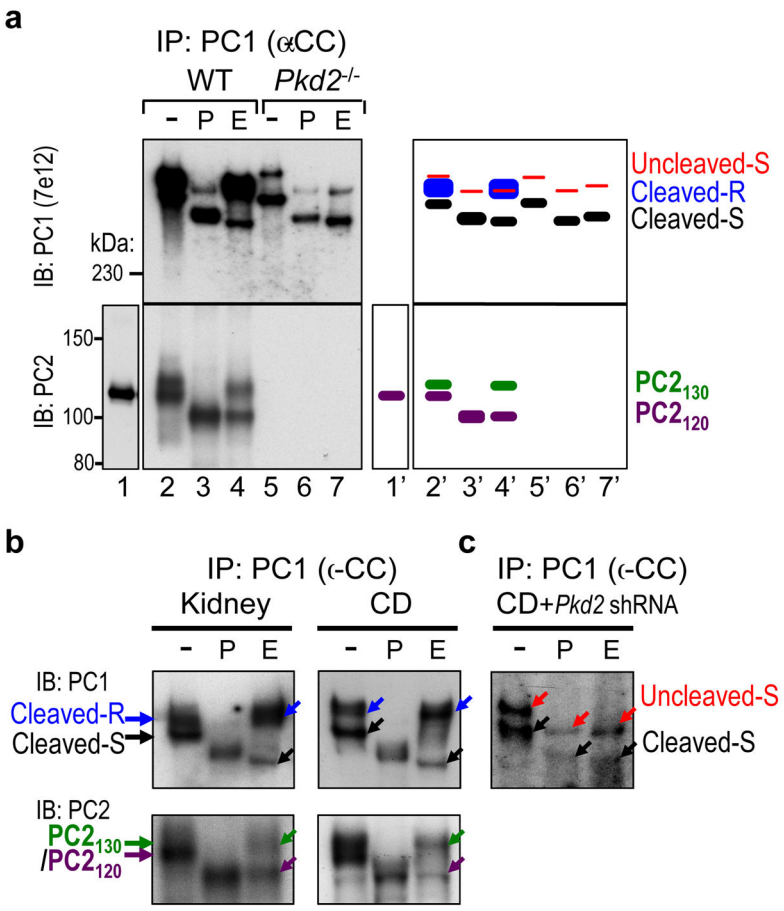

Figure 3.

Polycystin complex formation is required to reach the Golgi apparatus.(**a**) *N*-glycosylation analysis of endogenous polycystin complex in WT and *Pkd2*$^{-/-}$ MEFs. Polycystin complex was immunoprecipitated with anti-PC1 (α-CC), treated with PNGaseF (P) or EndoH (E), and analyzed by Western blot analysis with anti-PC1 (upper panel) or PC2 (lower panel). The schematic diagram at right provides an identification guide for various PC1 and PC2 forms, with color code that is maintained throughout the figures. Note that PC2 is co-immunoprecipitated from WT MEFs as EndoH-resistant $PC2_{130}$ and EndoH-sensitive $PC2_{120}$; and cleaved PC1 cannot acquire EndoH-resistance in *Pkd2*$^{-/-}$ MEFs. (**b**) *N*-glycosylation analysis of endogenous polycystin complex in kidneys (left) and CD cells (right) as in (**a**). Note that EndoH-resistant $PC2_{130}$ is detected in the polycystin complex in the kidney and CD lysates. (**c**) *N*-glycosylation analysis of polycystin complex in CD cells with *Pkd2* knockdown. Note that *Pkd2* knockdown prevented cleaved PC1 to acquire EndoH- resistance. EndoH-sensitive uncleaved PC1 (~520-kDa) is visible as in *Pkd2*$^{-/-}$ MEFs.

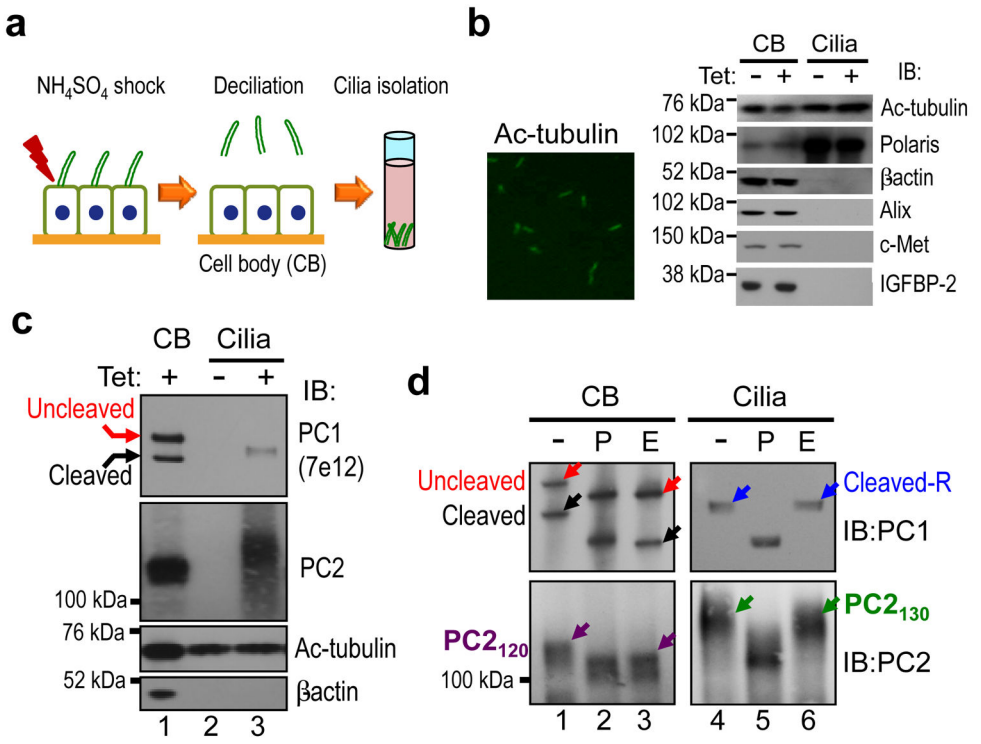

Figure 4.

Polycystin complex traffics to cilia through the Golgi apparatus.(**a**) Schematic diagram of cilium isolation from MDCK monolayers. (**b**) Visualization of intact cilia in the cilium preparation by immunofluorescence with anti-Ac-tubulin (left). Right panel shows the validation of the cilium preparations by Western blot analysis for marker proteins as indicated at right. The cilium preparation (Cilia) and the cell body (CB) without ("−") or with ("+") tetracycline induction were analyzed.(**c**) Western blot analysis of cilia isolated from un-induced ("−") and induced ("+") $MDCK^{PC1WT}$ cells with anti-PC1 or anti-PC2. (**d**) *N*-glycosylation analysis of ciliary PC1 and PC2 for the same sample as in (**c**). Parallel analysis of cell body (CB) served to identify cleavage status of ciliary polycystins. Note that only cleaved and EndoH-resistant PC1 and EndoH-resistant $PC2_{130}$ forms are present in cilia.

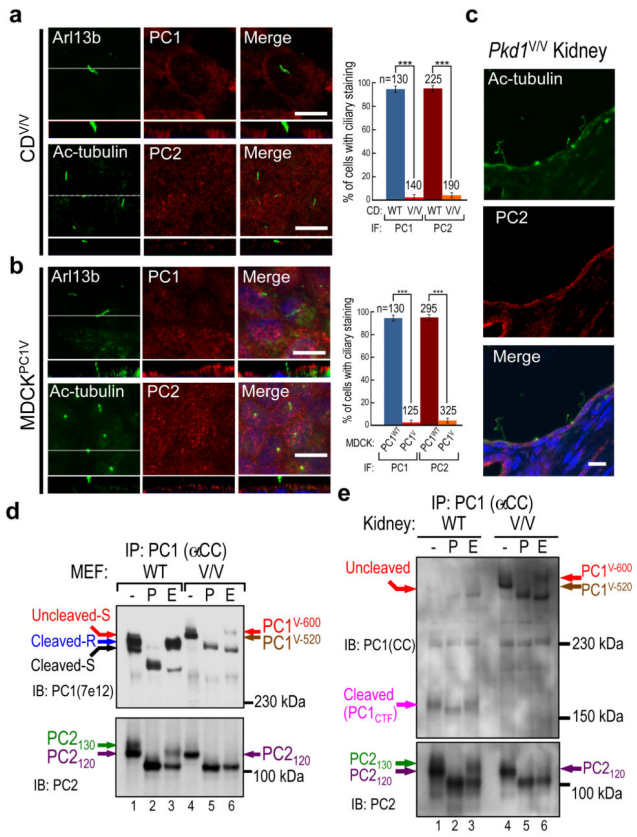

Figure 5.

GPS-cleavage is required for the ciliary trafficking of polycystin complex. (**a**) Confocal images of collecting duct cells isolated from *Pkd1*$^{V/V}$ kidneys (CD$^{V/V}$) stained with antibodies against PC1 (E4) or PC2. Arl13b or Ac-tubulin was used as a ciliary marker. The graph compares the percentage of cells with positive PC1 or PC2 in the wild-type CD (as shown in Fig. 1e or f) and CD$^{V/V}$ cells, from three independent experiments and presented as the mean ± SEM; *** $p<0.001$. The number of cells analyzed (n) is indicated. (**b**) Confocal images of induced MDCK^{PC1V} cells show absence of ciliary PC1^{V} and endogenous PC2. The graph compares the percentage of cells with positive PC1 or PC2 ciliary staining in MDCK^{PC1WT} (as shown in Fig. 2f) and MDCK^{PC1V} cells from three independent experiments, presented as the mean ± SEM; *** $p<0.001$. The number of cells analyzed (n) is indicated. The white line in the XY scan in (**a**, **b**) indicates the path of the XZ scan. Scale bar, 10 μm.(**c**) Confocal images of cystic collecting ducts of the *Pkd1*$^{V/V}$ kidney stained with anti-PC2. Note that PC2 was not detectable in 17 of 17 cilia analyzed. (**d**) *N*-glycosylation pattern of polycystin complex in *Pkd1*$^{V/V}$ MEFs versus wild-type MEFs. Polycystin complex was immunoprecipitated and analyzed as in Fig. 3, with PC1 and PC2 bands indicated with color code. Note that the co-precipitated PC2 from *Pkd1*$^{V/V}$ MEFs (lanes 4–6) was entirely EndoH-sensitive, lacking EndoH-resistant $PC2_{130}$ seen in wild-type MEFs (lanes 1–3). (**e**) *N*-glycosylation pattern of polycystin complex in *Pkd1*$^{V/V}$ kidney versus wild-type kidney. Polycystin complex was immunoprecipitated and analyzed as in (**d**), expect that anti-CC antibody was used to detect PC1. Note the presence of cleaved $PC1_{CTF}$ in wild-type kidney (lanes 1–3) but not in *Pkd1*$^{V/V}$ kidneys (lanes 4–6).

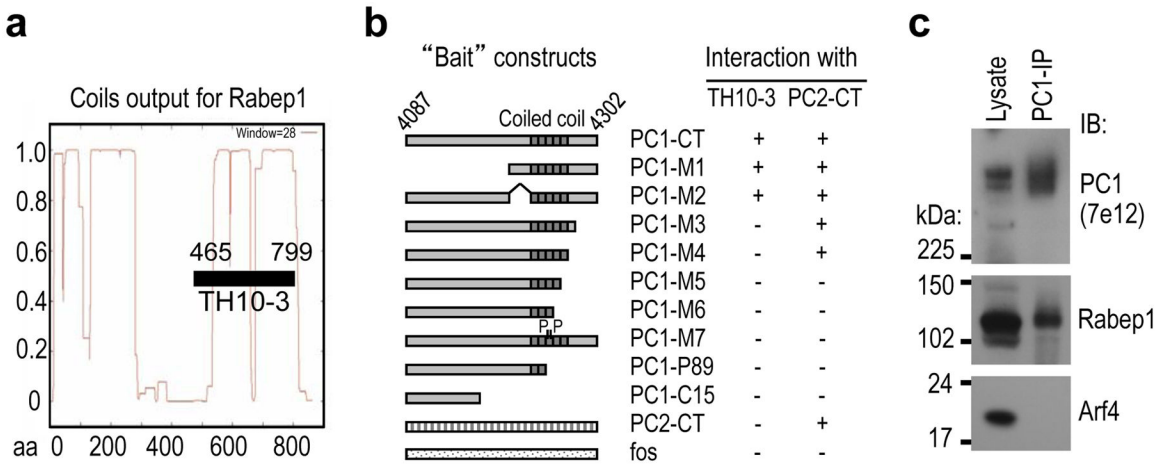

Figure 6.

Interaction of PC1 cytoplasmic C-terminal tail with Rabep1. (**a**) Yeast two-hybrid screening of a rat brain cDNA library using human PC1's 215-amino acid C-terminal tail as bait (PC1-CT) identified a clone(TH10–3) corresponding to amino acids 465 to 799 of Rabep1 with extensive coiled-coils[69]. (**b**) Mapping of Rabep1-interaction region by yeast two-hybrid assay using a series of PC1-CT deletion constructs[22]. The coiled-coil domain is indicated. PC1-M7 contains proline at *a* and *d* positions of the heptad, disrupting α-helical structure of the coiled-coil domain. PC1-P89 contains a germline mutation R4227X[22, 27]. PC1-C15 contains a somatic mutation found in a renal cyst resulting in reading-frame shift[22, 70]. Positive interaction was scored by both growth on triple selective medium and positive β-gal activity. PC2 C-terminal tail (PC2-CT) or fos served as negative controls. Interactions of the PC1 constructs with PC2-CT are shown as a comparison. (**c**) Co-immunoprecipitation of endogenous PC1 with Rabep1, but not with Arf4 in CD cells.

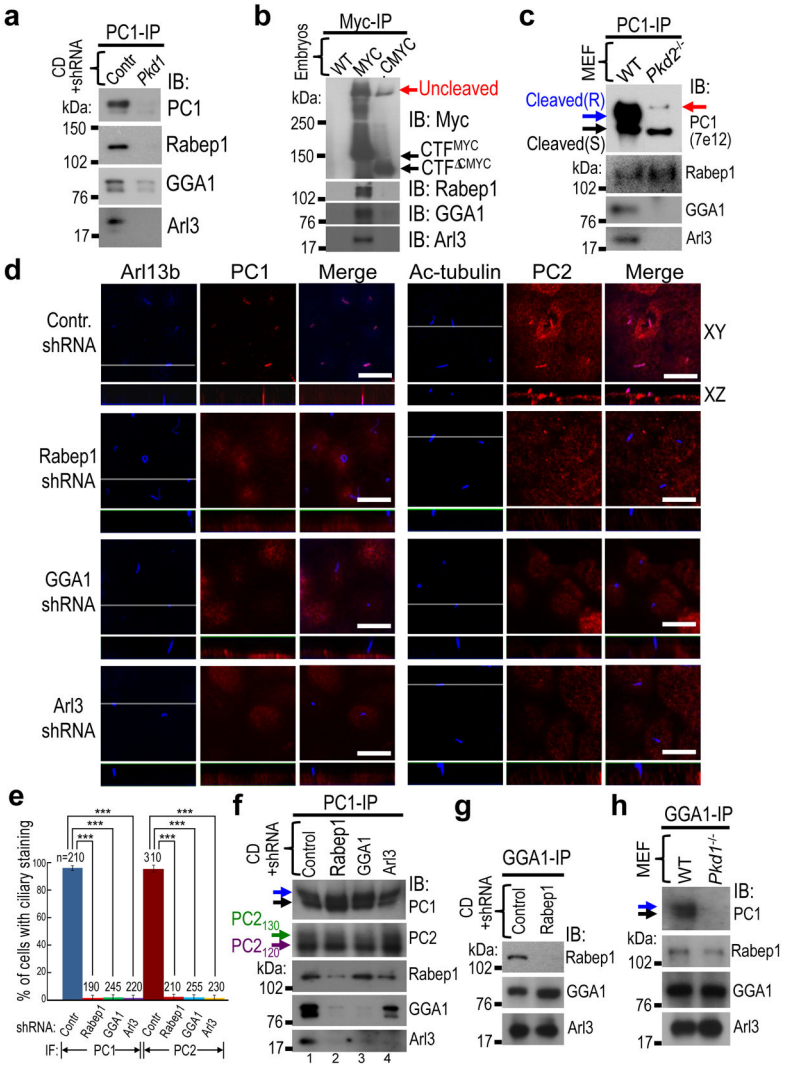

Figure 7.

Polycystin complex containing cleaved PC1 traffics to cilia through a Rabep1/GGA1/Arl3-dependent mechanism.(**a**) Co-immunoprecipitation of endogenous PC1 with Rabep1, GGA1 and Arl3 from CD cells. CD cells with shRNA-mediated *Pkd1* knockdown were used as a negative control. The larger areas of the blots are shown in Supplementary Fig. 3d. (**b**) Co-immunoprecipitation of C-terminal Myc-tagged PC1 with Rabep1, GGA1 and Arl3 from *Pkd1*$^{MYC/MYC}$ embryo lysates (MYC). *Pkd1*$^{\Delta_{CMYC/\Delta^{CMYC}}}$ knock out embryos that express estruncated PC1 lacking the C-terminal 257 aa (ΔCMYC) and untagged wild-type (WT) embryos were used as negative controls. (**c**)Wild-type (WT) or *Pkd2*$^{-/-}$ MEF cell lysates were immunoprecipitated with anti-PC1 (α-CC) and the IP products were analyzed with the antibodies as indicated.(**d**) Knockdown of Rabep1, GGA1, or Arl3 in CD cells abolishes ciliary localization of endogenous PC1 (left panels) and PC2 (right panels). The white line in the XY scan indicates the path of the XZ scan. For knockdown of each target protein, three shRNAs for Rabep1, four shRNAs for GGA1, and two shRNAs for Arl3 were used and each lentivirals hRNAs similarly inhibit the expression of the target proteins by ~90%

(Supplementary Fig. 3a–c). Scale bar, 10 μm. (**e**) Quantification of PC1 and PC2 ciliary localization in CD cells expressing various shRNAs in (**d**) was performed from four independent experiments and presented as the mean ± SEM; *** $p<0.001$.(**f**) Endogenous PC1 were immunoprecipitated with anti-PC1 (α-CC) from CD cells expressing the shRNA as indicated, and analyzed with various antibodies as indicated. Note that acquisitions of EndoH-resistance of PC1 and PC2 were not affected by any of the shRNAs. The larger areas of the blots are shown in Supplementary Fig. 3e. (**g**) Co-immunoprecipitation of native GGA1 and Arl3 in CD cells with Rabep1 knockdown. The specificity of the GGA1-Arl3 interaction was validated using CD cells with GGA1 knockdown (Supplementary Fig. 4d). (**h**) Co-immunoprecipitation of GGA1 with Rabep1 and Arl3 in both wild-type (WT) and *Pkd1*$^{-/-}$ MEFs.

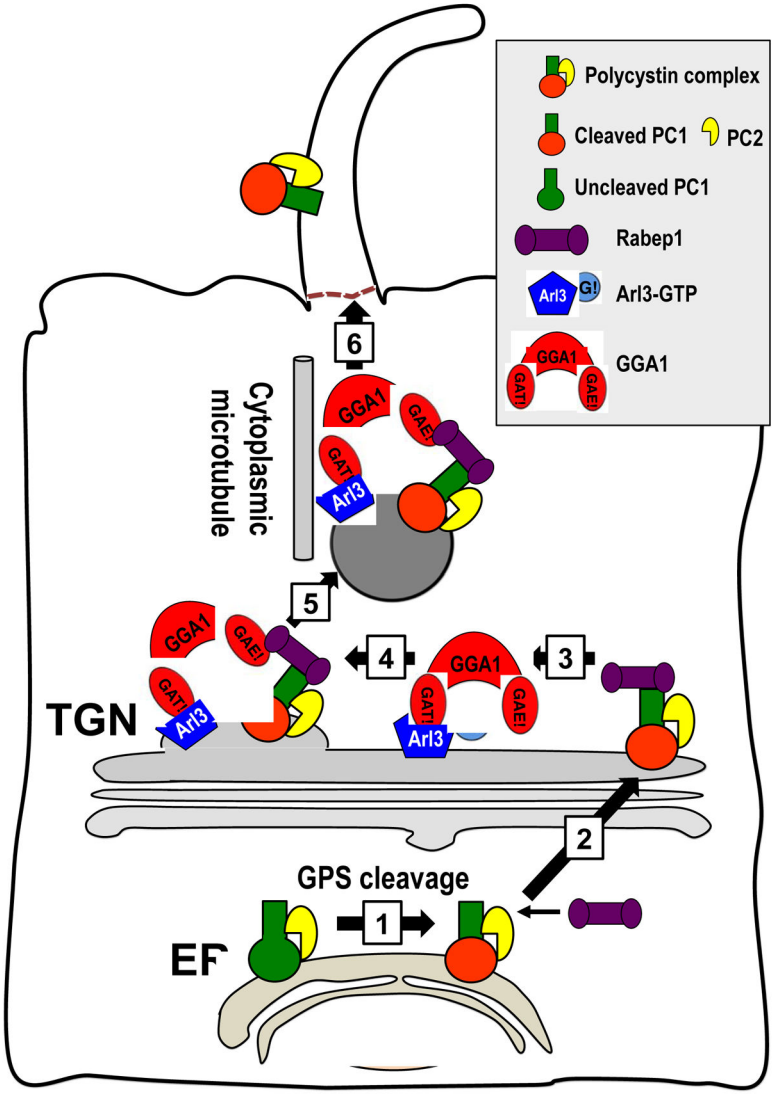

Figure 8.

Model for ciliary trafficking of the polycystin complex. PC1 is cleaved at GPS and forms a complex with PC2 in the ER (1). Rabep1 binds PC1's cytoplasmic C-terminal tail at a pre-Golgi compartment (2), and this complex traffics to the *trans*-Golgi network (TGN). At the TGN, Rabep1 couples the polycystin complex to a GGA1/Arl3 module (3), which is formed by Arl3-GTP binding to GGA1 *via* the GAT domain. GGA1 then assembles the clathrin coat (4) to form the vesicle carrier (5). The resulting polycystin complex-bearing vesicle traffics along the cytoplasmic microtubules to the base of cilia (6) and enters the cilium by an unknown mechanism.

Table 1

Stable MDCK cells with tetracycline-inducible expression of mouse PC1 proteins

MDCK cells	PC1 variant expressed	Description
$MDCK^{PC1WT}$	$PC1^{WT}$	Full-length wild-type PC1 with a C-terminal FLAG tag
$MDCK^{PC1–2M}$	$PC1^{2M}$	Full-length PC1 with a C-terminal FLAG tag, containing amino acid substitutions at L4219P and A4222P within the coiled-coil domain
$MDCK^{PC1-R/X}$	$PC1^{R/X}$	PC1 terminating at R4218X with a C-terminal FLAG tag before the stop codon
$MDCK^{PC1V}$	$PC1^{V}$	Full-length PC1 with a C-terminal FLAG tag, containing amino acid substitution T3041V at GPS cleavage site